19th Australasian Tunnelling Conference – Acosta-Martínez, Stewart and Hudson-Smith (Eds.)

Effects of in-situ principal stress magnitudes on unloading strength

A. Rooz & B. Sainsbury
School of Engineering, Deakin University, Waurn Ponds, Australia

ABSTRACT: Rock strength is a crucial parameter in underground excavation design, typically assessed under compressional (loading) conditions, termed here as loading strength. However, excavation redistributes in-situ stresses–particularly reducing the minor principal stress–resulting in unloading mechanical behaviour. In this excavation-induced stress regime, the geomechanical response of rock differs from its compressional response and can be referred to as its unloading strength (post-excavation strength). In-situ stress states naturally vary in principal stress magnitude ratios due to geological, structural, and tectonic factors. This study investigates the effect of these stress ratios on unloading strength and compares it to conventional loading strength. Laboratory tests on Adelaide black granite show that unloading strength is consistently lower than loading strength, with the reduction significantly influenced by in-situ principal stress ratios. An empirical relationship is proposed to characterise the unloading strength for the granite and unloading paths tested. The findings demonstrate the importance of incorporating unloading strength to capture softening behaviour in underground excavation design.

1 INTRODUCTION

The safety and stability of underground excavations depend greatly on mechanical properties of the host rock, particularly its strength. The rock mass strength response is strongly influenced by the pre-excavation in-situ stress state and the stress path it undergoes. This response differs significantly between loading (compressional stress path) and unloading (typical eventual excavation-induced stress path). Understanding in-situ stress conditions, typical excavation stress paths, and their influence on rock behaviour is essential for managing and maintaining stability in rock engineering applications (Guo et al. 2024). Typical loading and unloading stress paths are illustrated in Figure 1.

Rock mass near an excavation face will always experience a reduction in the minor principal in-situ stress (σ_3). In more complex cases, the major principal in-situ stress (σ_1) may simultaneously increase, or a series of unloading-loading (complex) combinations may occur.

The magnitude of in-situ stress is influenced by multiple factors, including depth, rock type (lithology), and plate tectonics. Brown & Hoek (1978) analysed 120 stress measurement data points to establish relationships between depth (z, in meter), the stress ratio (k , the ratio of horizontal to vertical stress), and vertical stress (σ_v). Subsequent studies, such as Hudson & Harrison (1997), have shown that localised structurally related stresses can significantly exceed those predicted by gravitational and tectonic components alone. Therefore, incorporating realistic and site-specific stress conditions into experimental design and testing is essential to obtain meaningful predictions of rock mass behaviour.

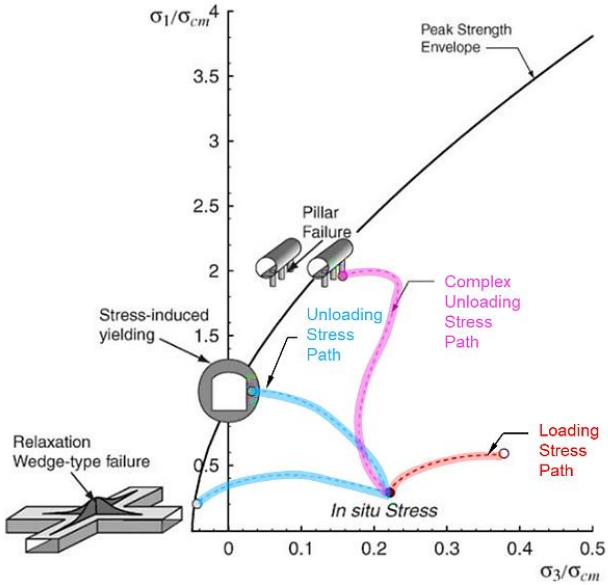

Figure 1. Generalised stress paths during underground excavation (modified after Martin et al. 2003).

In most conventional loading laboratory experiments (e.g., Uniaxial Compressive Strength (UCS) and Triaxial Compressive Strength (TCS) tests), specimens start in a stress-free state (zero confinement), with load applied solely in one direction until failure. In contrast, in-situ rock exists in a state of equilibrium under triaxial stress conditions. During excavation, at least one principal stress component decreases, meaning the stress path in conventional loading tests significantly differs from the actual conditions experienced by the rock. Unloading tests are therefore recommended to better replicate in-situ stress changes and provide more representative rock response data for design (Vervoort 2024).

This study investigates the strength response of Adelaide black granite (ABG) through a series of loading and unloading tests, comparing post-excavation rock strength with conventional compressive strength and evaluating the effect of in-situ principal stress magnitudes. A total of five specimens have been tested for UCS (loading) and nine for TCS (six loading and three unloading).

2 EXPERIMENTAL DESIGN

2.1 *Specimen Preparation and Testing Systems*

A total of 14 cores have been recovered from a slab of ABG and prepared by trimming and grinding both ends to produce standard cylindrical specimens with a diameter-to-height ratio of 1:2 (54 mm × 108 mm), ensuring parallel and perpendicular surfaces. Figure 2 shows the drilled slab and a prepared specimen ready for testing. Full details on sample preparation and characterisation of ABG can be found in Rooz & Sainsbury (2025).

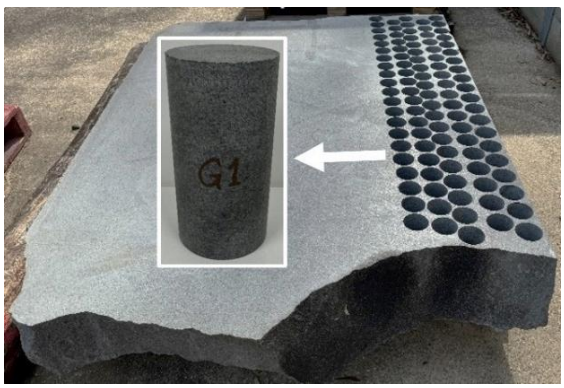

Figure 2. Slab of Adelaide black granite and a representative prepared specimen.

2.2 *Establishment of In-situ Principal Stress Magnitudes*

In lieu of site-specific stress measurements, in-situ stresses can be estimated using Figure 3a, which compiles geostress data from various regions worldwide, including Australia, Canada, USA, Southern Africa, Scandinavia, and others (Brown & Hoek 1978). From these data, a trend line yields the empirical Equation 1 for estimating vertical stress.

$$\sigma_v = 0.027\, z \quad (1)$$

Common excavation depths for underground tunnelling and mining projects range from a few hundred meters to approximately 1500 m, depending on geological conditions and project requirements. For this study, vertical stresses at three depths (z = 500, 1000, and 1500 m) have been considered, giving estimated σ_v values of 14, 28, and 42 MPa, respectively, using Equation 1.

The ratio of in-situ principal stress magnitudes (k-value) can be determined using Equation 2, where σ_h represents horizontal (or lateral) stress.

$$k = \frac{\sigma_h}{\sigma_v} \quad (2)$$

Figure 3b shows the geostress distribution in terms of the k-value. Due to the limitations of the laboratory triaxial system, k-values greater than 1 cannot be reproduced experimentally. As such, k-values of 1, 1/2, and 1/3–corresponding to underground points A, B, and C in Figure 3b–have been selected for testing.

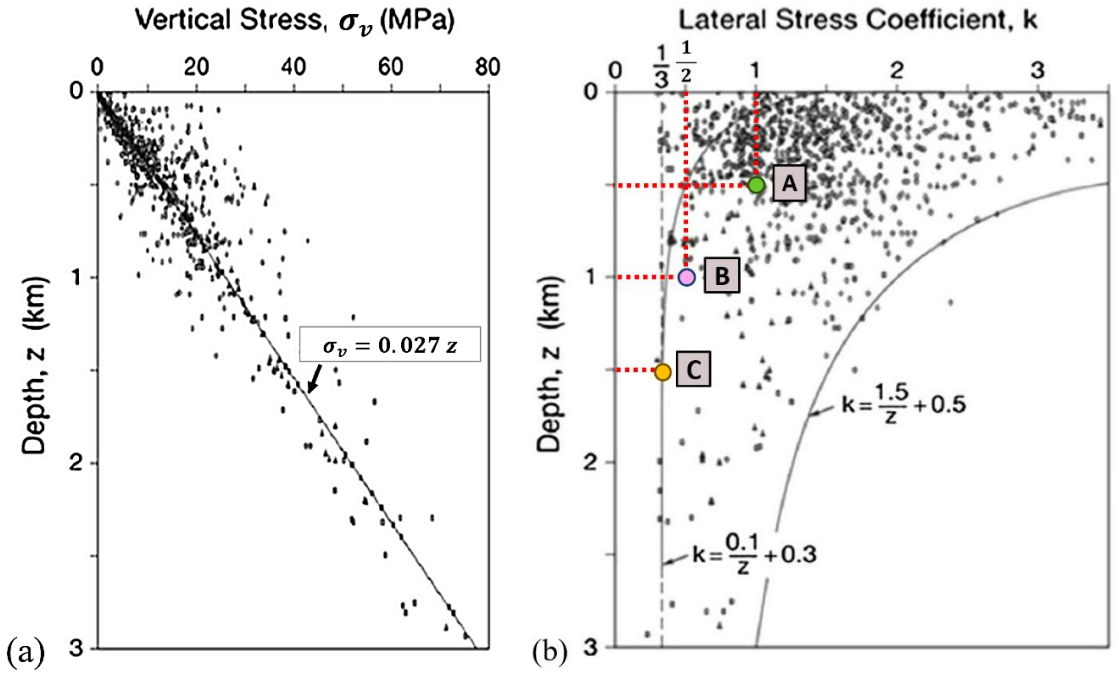

Figure 3. Distribution map of measured geostress data with depth variation: (a) Vertical stress magnitudes; (b) Lateral stress coefficient [modified after Brown & Hoek (1978)].

The horizontal stress has been estimated to be 14 MPa using Equation 2 and kept constant for all tests presented in this study.

2.3 *Testing stress paths*

To determine the conventional strength properties of ABG, two loading stress paths (L1 and L2) have been simulated in the laboratory, as illustrated in Figure 4a. Stress path L1 corresponds to unconfined and zero confining pressure (CP) conditions, while stress path L2 represents triaxial testing with a CP (σ_3) of 14 MPa.

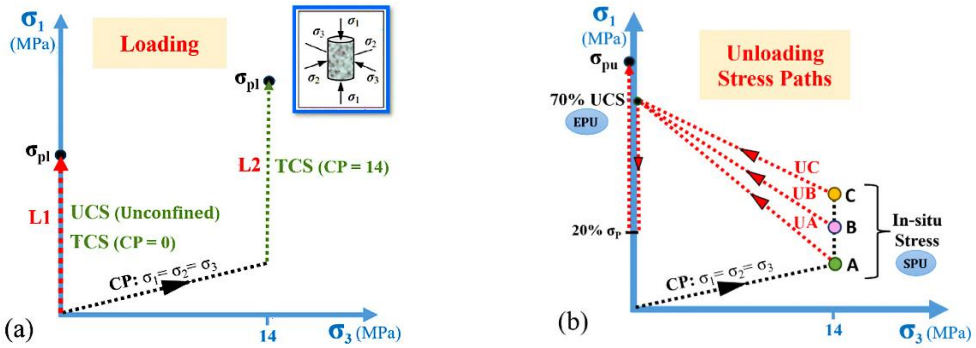

Figure 4. Testing stress paths: (a) Loading in UCS and TCS tests; (b) Unloading, representing excavation-induced stress at depths of A, B, and C.

As shown in Figure 4b, to determine unloading (post-excavation) strength, first the in-situ stresses at points A, B and C (Figure 3b) have been applied, representing the in-situ stress before excavation (pre-excavation stress state). This stress state is referred to as the Starting Point of Unloading (SPU). Once the SPU has been reached, the unloading stress paths of UA, UB or UC have been followed in the triaxial machine to simulate excavation. For each case, the sample reached the same Ending Point of Unloading (EPU) stress, corresponding to 70% of the UCS loading value. This 70% axial stress level has been chosen at the EPU in accordance with previous unloading studies on granite (Alejano et al. 2017, Duan et al. 2019) and represents a value that has exceeded the damage (crack) initiation threshold (Kaiser & Kim, 2015, Bewick 2021), at which spalling failure can be expected (Figure 6). Once zero CP conditions have been reached, the axial stress (σ_1) has been reduced to 20% of the loading strength, representing the lower limit of the elastic zone. Reloading has subsequently been applied until specimen failure to determine the unloading strength and stiffness response (post-excavation strength). Note the stiffness responses are not reported in this study. All tests have been conducted at a constant rate of 0.1 MPa/s.

3 STRENGTH RESULTS AND ANALYSIS

3.1 *Loading strength*

Table 1 presents the average peak loading strength (σ_{pl}) of five completed tests in UCS and three TCS tests conducted at CP = 0 MPa. The triaxial tests have been conducted at 0 MPa CP to confirm the accuracy of the machine and testing procedure, as well as to characterise the volumetric response, which is difficult to capture in a UCS test (Crouch 1970).

Table 1. Loading strength of Adelaide black granite specimens.

Test type	Samples Tested	σ_3 (MPa)	Average σ_{pl} (MPa)
Unconfined Compressive Strength	5	-	246.4
Triaxial Compressive Strength	3	0	244.3
	3	14	414.4

The average loading strength of three tests conducted under stress path L2 (σ_3=14 MPa) has been determined to be 414.4 MPa. The intact compressional response of ABG is represented in Figure 6 as the 'Intact Strength Envelope'.

3.2 *Unloading strength*

Unloading strength refers to the post-excavation strength. Table 2 summarizes the peak unloading strength (σ_{pu}) for each specimen tested. This value represents the stress required to fail the sample

after simulated stress unloading. The loading and unloading strengths are compared in Figure 5, with respect to k-values.

Table 2. Unloading strength of Adelaide black granite specimens at different in-situ principal stress ratios (k-values).

Simulated In-Situ Conditions (SPU)				Simulated Unloaded Conditions (EPU)			Measured σ_{pu} (MPa)
Representative depth (m)	k	σ_1 (MPa)	σ_3 (MPa)	Stress path	σ_1 (MPa)	σ_3 (MPa)	
500	1	14	14	UA	171	0	187.8
1000	1/2	28	14	UB	171	0	220.5
1500	1/3	42	14	UC	171	0	236.6

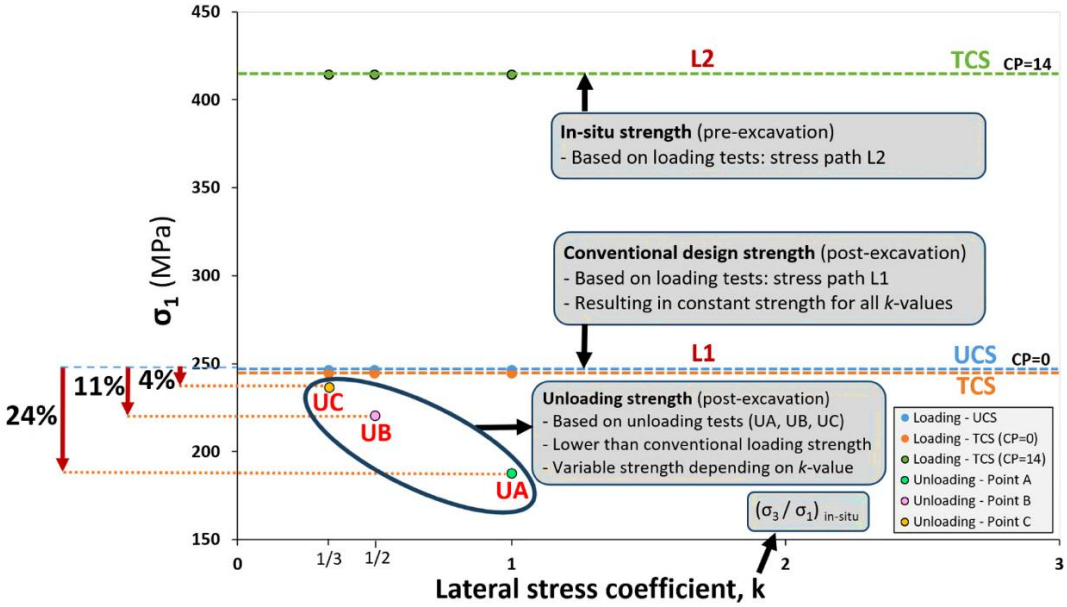

Figure 5. Comparison of loading strengths (points on L1 and L2 dashed lines) and unloading strength magnitudes (UA, UB, UC) of Adelaide black granite specimens at underground locations A, B, and C, with respect to in-situ principal stress ratios (k-values).

The strengths obtained from the unloading tests, shown in Figure 6, are presented with respect to the minor principal stress (σ_3) and compared against the loading strength for intact ABG rock. Their percentage change from their loading response is also presented.

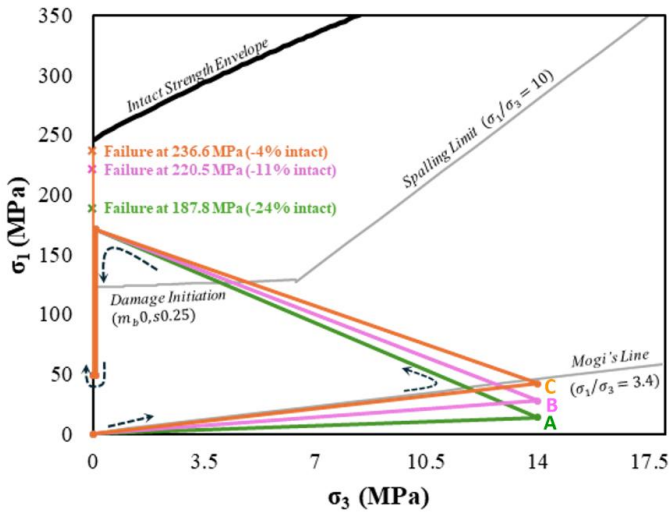

Figure 6. Comparison of unloading strength and loading strength magnitudes of Adelaide black granite specimens at underground locations A, B, and C, with respect to minor principal stress.

From the analysis, the following key conclusions can be drawn.

- All unloading strengths measured are lower than the loading strengths at zero CP. This result suggests that using the loading strength for design overestimates the rock's actual strength in-situ. In practical terms, damage induced on the rock during the unloading process must be considered in the design material strength. This is usually achieved via a strain-softening numerical approach (Rudnicki & Rice 1975).
- The degree of strength deterioration depends on the in-situ stress (pre-excavation) and the unloading stress path. For example, unloading from stress point A, where the principal in-situ stress ratio is greater (k = 1), resulted in significantly lower unloading strength (24% lower than the loading strength). Even unloading from stress point B led to a notable strength reduction (11%). This significant reduction can be attributed to the greater rate of change in σ_1 relative to σ_3 (i.e., the longer unloading path to reach the EPU). This phenomenon has been previously described by Board et al. (2001) related to seismicity.

Figure 7 presents unloading strength ($\sigma_{pu} = \sigma_{p\ (post\text{-}excavation)}$), expressed as a percentage of the loading strength ($\sigma_{pl} = UCS$). This figure relates the ratio of principal stress changes before and after unloading ($\Delta\sigma_1/\Delta\sigma_3$) to the degree of accumulated damage. The 'accumulated damage' (i.e. unloading damage) refers to the percentage reduction in strength from the intact condition (UCS) to the post-excavation condition. This reduction can be quantified using Equation 3:

$$Unloading\ damage\ (\%) = \left(1 - \frac{\sigma_{p\ (post-excavation)}}{UCS}\right) \times 100 \quad (3)$$

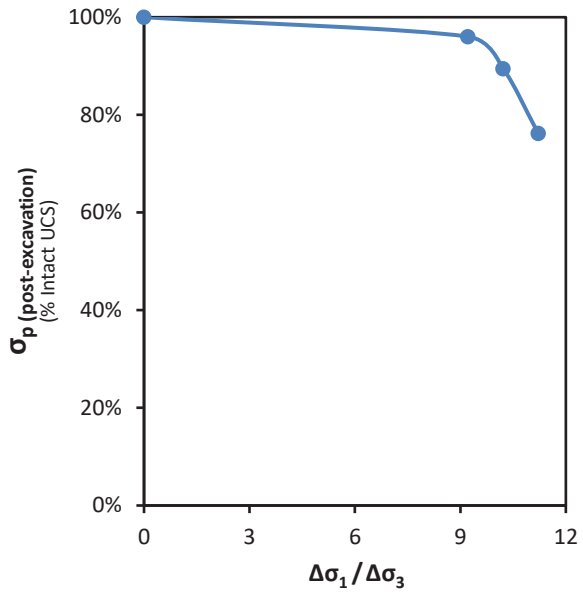

Figure 7. Relationship between changes in principal stress magnitudes from in-situ to final (post-excavation) states ($\delta\sigma_1/\delta\sigma_3$) and post-excavation strength, illustrating accumulated damage.

A relationship can be established to describe the post-excavation design strength (σ_p) in MPa for the stress paths simulated in the ABG, as presented in Equation 4.

$$\sigma_{p\ (post-excavation)} = \frac{UCS}{100}\left[-0.0025\ .\ e^{\left(0.8196 \times \frac{\Delta\sigma_1}{\Delta\sigma_3}\right)} + 100\right] \quad (4)$$

Where *UCS* is measured by the conventional approach (in MPa). $\Delta\sigma_1$ and $\Delta\sigma_3$ represent the differences in principal stresses between EPU ($\sigma_1 = 70\%\ \sigma_p$, $\sigma_3 = 0$) and SPU (in-situ stresses). In the conducted unloading tests, $\sigma_1$increased from 14 (or 28 or 42) to 171 MPa, while σ_3 decreased from 14 to 0 MPa. The values in Equation 4 are adjusted based on Figure 7 to account for percentage damage.

This equation enables estimation of post-excavation (design) strength using only conventional UCS value, without the need to perform unloading tests. However, it has been derived exclusively for ABG and should not be applied to other rock types without further validation.

4 DISCUSSION

Through the application of Equation 3, the problem with conventional techniques used to estimate strength damage in a rock sample are resolved. For instance, the designer no longer needs to estimate plastic strain (Martin & Chandler 1994), complete complex laboratory testing (Guo et al. 2025), or conduct complex simulations (Hajiabdolmajid et al. 2002) in order to quantify the post-excavation strength that should be applied in the design solution. Instead, the strength can be directly estimated based on the UCS and change in in-situ principal stress magnitudes and then applied in analytical design solutions.

However, these outcomes are generalised for Adeliade black granite (a strong and brittle rock) and under a specific loading and unloading stress path. The results should be further explored for a wider range of rock types (sedimentary, metamorphic, and igneous) with varying *UCS* values. Additionally, investigations should consider different stress conditions (in-situ: σ_1 and σ_3), k-value, intact unconfined modulus (E_i), intact confined modulus (E_{ic}), or the modulus ratio ($MR = E_i/UCS$). Future studies should examine the effects of different stress paths (pure unloading only or loading-unloading combinations), unloading rates and anisotropy. A generalized empirical formula incorporating these factors could enhance the characterisation of intact rock softening behaviour under unloading stress conditions.

5 CONCLUSIONS

In underground excavation design, rock strength is a key parameter that engineers rely on. This study investigates rock strength, commonly obtained from UCS test, and compares it with unloading tests that account for excavation effects. For this purpose, Adelaide black granite specimens have been provided and prepared for testing.

The results show that unloading strength is persistently lower than loading strength, particularly at locations with lower major principal in-situ stress magnitudes (or higher k-value). For instance, at point A, representing 500 meters underground, the unloading strength was significantly reduced by 24%. The importance of conducting unloading tests lies in their ability to incorporate in-situ stress conditions, considering factors such as depth, principal in-situ stress ratio, and unloading stress–factors that are often overlooked in conventional loading tests, including UCS (unconfined) and TCS (confined with zero CP).

Although loading tests are significantly simpler and faster approach than unloading tests, they tend to overestimate rock strength after excavation and provide a single strength value for varying underground conditions. Real-world excavation sites may exhibit different in-situ stress conditions (e.g., points A, B, and C). Relying solely on loading strength assumes uniform conditions, which may not accurately represent the actual stress distribution. Unlike conventional loading tests, which do not account for excavation-induced stress changes, unloading tests simulate more realistic stress conditions encountered in underground excavations.

By incorporating triaxial in-situ stress conditions and excavation-induced stress paths, unloading tests provide a more accurate assessment of rock behaviour under actual geological conditions. Therefore, considering unloading effects is crucial for excavation design, underground support, and financial planning in engineering projects.

6 REFERENCES

Alejano, L.R., Arzúa, J., Bozorgzadeh, N. & Harrison, J.P. 2017. Triaxial strength and deformability of intact and increasingly jointed granite samples. *International Journal of Rock Mechanics and Mining Sciences* 95: 87–103.

Bewick, R.P. 2021. The Strength of massive to moderately jointed rock and its application to cave mining. *Rock Mechanics and Rock Engineering* 54(8): 3629–61.

Board, M., Brummer, R. & Seldon, S. 2001. Use of numerical modelling for mine design and evaluation. *Underground Mining Methods: Engineering Fundamentals and International Case Studies; Society for Mining, Metallurgy and Exploration*, Littleton, Colorado, USA, 483–92.

Brown, E.T. & Hoek, E. 1978. Trends in relationships between measured in-situ stresses and depth. *International Journal of Rock Mechanics and Mining Sciences & Geomechanics Abstracts* 15(4) 211–5.

Crouch, S.L. 1970. Experimental determination of volumetric strains in failed rock. *International Journal of Rock Mechanics and Mining Sciences & Geomechanics Abstracts* 7(6): 589–603.
Duan, K., Ji, Y., Wu, W. & Kwok, C.Y. 2019. Unloading-induced failure of brittle rock and implications for excavation-induced strain burst. *Tunnelling and Underground Space Technology* 84: 495–506.
Guo, J., Ma, L., Liu, Z. & Wang, S. 2024. The influence of mining stress paths on rock damage and permeability. *Environmental Earth Sciences* 83(10): Article No. 307.
Guo, S., Qi, S., Zhang, S., Waqar, M.F., Xiong, F., Liang, N., Zheng, B., Ma, X. & Tang, F. 2025. A two-parameter damage-controlled strength model to predict the fracturing of brittle rock mass at great depth. *Case Studies in Construction Materials* 23: Article No. e05028.
Hajiabdolmajid, V., Kaiser, P.K. & Martin, C.D. 2002. Modelling brittle failure of rock. *International Journal of Rock Mechanics and Mining Sciences* 39(6):731-41.
Hudson, J.A. & Harrison, J.P. 1997. *Engineering Rock mechanics An Introduction to the Principles*. Elsevier Science.
Kaiser, P.K. & Kim, B.H. 2015. Characterization of strength of intact brittle rock considering confinement-dependent failure processes. *Rock Mechanics and Rock Engineering* 48(1): 107–19.
Martin, C.D. & Chandler, N.A. 1994. The progressive fracture of Lac du Bonnet granite. *International Journal of Rock Mechanics and Mining Sciences & Geomechanics Abstracts* 31(6): 643–59.
Martin, C.D., Kaiser, P.K. & Christiansson, R. 2003. Stress, instability and design of underground excavations. *International Journal of Rock Mechanics and Mining Sciences* 40(7–8): 1027–47.
Rooz, A.F.H. & Sainsbury, B.A. 2025. Adelaide black granite: geomechanical characterisation for underground design. *Australian Journal of Earth Sciences* 72(2): 233–51.
Rudnicki, J.W. & Rice, J.R. 1975. Conditions for the localization of deformation in pressure-sensitive dilatant materials. *Journal of the Mechanics and Physics of Solids* 23(6): 371–94.
Vervoort, A. 2024. In situ stress paths applied in rock strength characterisation result in a more correct and sustainable design. *Sustainability* 16(11): Article No. 4711.